Smart Structures and Systems, *Vol. 27, No. 4 (2021) 691-703*
DOI: https://doi.org/10.12989/sss.2021.27.4.691

A developed model predictive control scheme for vibration attenuation of building structures

Afshin Bahrami Rad [1], Mahdi Nouri [1], Javad Katebi*[2] and Seyyed Arash Mousavi Ghasemi [1]

[1] *Department of Civil Engineering, Tabriz Branch, Islamic Azad University, Tabriz, Iran*
[2] *Faculty of Civil Engineering, University of Tabriz, Tabriz, Iran*

(*Received July 11, 2020, Revised November 10, 2020, Accepted November 19, 2020*)

Abstract. Model predictive control (MPC) is an optimal control algorithm in which the current control action is obtained by solving an optimization problem in the presence of hard and soft constraints in the finite time horizons sequentially. In most cases, neglecting the effects of the external loads in predicting the future responses of the structures lead to inaccurate control action. Therefore, it could be beneficial to consider the effects of external loads in the future within the MPC to improve its accuracy. In this paper, a developed model predictive control (DMPC) scheme is introduced. For this purpose, a forecasting seismic excitation model is formulated by two sequential autoregressive (AR) models. One of those estimates the future output of the seismic excitation and the second one enhances the estimation accuracy. Then, the efficiency of the presented approach is demonstrated by the numerical study of two benchmark buildings equipped with an active tuned mass damper (ATMD). The performance of the proposed MPC is finally compared with the conventional and ideal MPCs. The numerical outputs prove the competency and higher conformity of the proposed MPC with the ideal one almost in all of the cases. Twelve benchmark performance indices are also utilized for determining the superiority of the method. The average conformity values for all of the performance indices for the proposed method in the three- and nine-story buildings are by up to 17.75% and 9% more than the values in conventional one, respectively.

Keywords: model predictive control; vibration attenuation; seismic excitation; autoregressive model; active mass damper

1. Introduction

Seismic control of structures with new control system using different control algorithms such as classic, optimal, stochastic, and robust has always been of interest to many researchers (Pnevmatikos and Gantes 2011, Pnevmatikos 2012, Gharebaghi and Zangooeia 2017, Katebi and Zamen 2018, Moghaddasie and Jalaeefar 2019, Katebi and Jangara 2020). In most of the optimal control algorithms, an optimization problem is solved in an infinite time-horizon to achieve the optimal control rule. Model predictive control (MPC) in contrast is a subset of optimal control algorithms in which the optimization problem is solved sequentially in the finite time horizons while considering current and future time slots simultaneously (Wang 2009).

Due to its considerable advantages, MPC is one of the most interesting control methods in many fields. Its application in civil engineering is also a common issue. In Mei *et al*. (2001), a combination of the MPC and the Feedforward–Feedback (FF-FB) strategy was employed to control the structural responses under the seismic excitations. In another study, an MPC scheme with acceleration feedback was formulated in structural control under earthquake excitations (Mei *et al*. 2002). A model predictive control strategy was proposed for protection of structures during earthquakes in Xu and Li (2011). A hybridized model predictive control and sliding mode control was also investigated for active vibration suppression of a 1D piezoelectric bimorph structure in Kim *et al*. (2013).

The application of the MPC scheme in the vibration control of wind-excited tall buildings has also been studied (Mei *et al*. 2004). A robust MPC scheme was obtained based on state trajectory sensitivity against uncertain parameters in Lana and Rotea (2008). A modified MPC approach was formulated with the partial-state concept of direct output feedback (DOF) to reduce the number of sensors for real implementation in Yang *et al*. (2011). A novel fast model predictive control method was presented to protect the large-scale engineering structures from natural hazards in Chen *et al*. (2017). In Peng *et al*. (2017), a novel fast model predictive control regarding actuator saturation was proposed for large-scale structures. In another study, two practical MPC algorithms with multi-input delay were developed for vibration control of large-scale structures in Peng *et al*. (2018). A novel distributed MPC method based on a substructuring technique for smart tensegrity structure vibrations was proposed in Peng *et al*. (2020).

Model predictive control is a model-based control approach in which the accuracy of the controller is highly dependent on the accuracy of the system model (Khodabandehlou *et al*. 2018) so, it is essential to have a

*Corresponding author, Associate Professor,
E-mail: jkatebi@tabrizu.ac.ir

ISSN: 1738-1584 (Print), 1738-1991 (Online)

model with least imperfection. But, it is often difficult to estimate the model of the systems properly. Therefore, the estimated model contains uncertainties. To tackle the problem some concepts including stochastic MPC (Farina *et al*. 2016, Mayne 2016, Mesbah 2016, Heirung *et al*. 2018, Seron *et al*. 2019) and robust MPC (Lee 2014, Luo *et al*. 2017, Patan 2018) have been introduced accordingly. The aim of both concepts is considering the uncertainty impacts on the control process of systems. Generally, the model uncertainty is generated from two main origins: (1) unmodelled dynamics of a plant; (2) unmeasured noise/ disturbances which enter the plant (Patan 2018).

Since the MPC doesn't consider the applied external load effects in the prediction and the control process of the structures, estimating the applied future loads to the structures may attenuate the model-based uncertainties. In other words, given the MPC configuration in which the control law is calculated based on predicting the system behavior in the future steps, therefore, the possibility of predicting the external loads applied to the system in the future steps can also be effective in determining the control law more accurately. But the external loads applied to the system are not easily predictable because of their stochastic nature. Therefore, providing a solution that can be used to predict the external loads applied to the system simultaneously with predicting the system responses in the MPC process can significantly increase the accuracy of the desired control algorithm.

The main contribution of this paper is to present a new developed version of MPC scheme considering seismic excitation predictive term (section 4) in the obtained control rule. The seismic excitation predictive term is also obtained in two stages. In the first stage, an AR model is formed based on past measured ground acceleration, and in the second one, another AR model is established based on the error between measured and the obtained predicted states from the first stage. Then, the AR models are integrated and utilized in the primary model as a compensator for a part of the uncertainty. It is worth noting that, Recursive Least Squares (RLS) method is used for both the parameter determination of the AR models and the noise elimination of measured ground acceleration. Furthermore, the Kalman Filter (KF) is used as an optimal estimator for the state estimation of the model in a full state manner. Actuator saturation is also considered defining hard control force constraints in the cost function. The numerical simulation of two benchmark buildings (three- and nine-story buildings) equipped with an active mass damper located on the top story under the four benchmark earthquake records (El Centro, Hachinohe, Northridge, and Kobe) is accomplished to evaluate the proposed control strategy.

In this paper, the cost function of the MPC is minimized subject to the control force constraints. Then, the proposed method is applied to the numerical study of a benchmark building. The performance and capability of the proposed method are finally compared with conventional MPC.

The paper is arranged as follows. The problem formulation is introduced in section 2. In section 3, a brief formulation for the conventional MPC is proposed. Section 4 is divided into three parts, in the first part, the formulation of seismic excitation model and in the second and third parts, Kalman Filtering and RLS methods are proposed, respectively. Then, at the end of this section, the proposed step-by-step algorithm is unveiled. In section 5, two numerical examples including, two benchmark buildings, are introduced to study. Section 6 contains some simulation results. The paper closes with a conclusion in section 7.

2. Problem formulations

A building equation of motion with ATMD under the seismic excitation is as follows

$$M\ddot{q} + C\dot{q} + Kq = \gamma u - \delta\ddot{x}_g \tag{1}$$

Where M, C, and K are $n \times n$ matrices of mass, damping and stiffness matrices, respectively; q, $\dot{q}$ and $\ddot{q}$ are $n \times 1$ vectors of displacement, velocity and acceleration vectors relative to the ground; γ of $n \times 1$ is the actuator location vector; δ of $n \times 1$ is coefficient vector for earthquake ground acceleration; u is the control force; $\ddot{x}_g$ is the ground acceleration. The state space format of the Eq. (1) is expressed as follows

$$\begin{aligned} &= \tilde{A}X + \tilde{B}_u u + \tilde{B}_r \ddot{x}_g \\ \dot{X} &= \begin{bmatrix} \dot{q} \\ \ddot{q} \end{bmatrix} = \begin{bmatrix} 0 & I \\ -M^{-1}K & -M^{-1}K \end{bmatrix} \begin{bmatrix} q \\ \dot{q} \end{bmatrix} \\ &\quad + \begin{bmatrix} 0 \\ M^{-1}\gamma \end{bmatrix} u + \begin{bmatrix} 0 \\ M^{-1}\delta \end{bmatrix} \ddot{x}_g \\ Z &= C_c \times X \end{aligned} \tag{2}$$

Where C_c of $2n \times 2n$ is the state-to-output matrix. The discrete time format of the Eq. (2) is expressed as

$$\begin{aligned} x_{k+1} &= Ax_k + Bu_k + G\ddot{x}_{g_k} \\ y_k &= C_d \times x_k \end{aligned} \tag{3}$$

Where $A = e^{\tilde{A}t}$, $B = P_1\widetilde{B_u}$ and $G = P_1\widetilde{B_r}$ for which $P_1 = \int_0^t e^{\tilde{A}\epsilon}\, d\epsilon$, x of $2n \times 1$ is system state, A of $2n \times 2n$ is state matrix, B and G of $2n \times m$ is the input-to-state matrix, u of $m \times 1$ is input or control vector, y of $2n \times 1$ is output vector, C_d of $2n \times 2n$ is the state-to-output matrix, k stands for discrete-time step index and t is sampling time.

3. Model predictive control

Model predictive control, also known as receding-horizon control, is the online solving of finite- horizon optimal control problems with constraints on states and control inputs. The obtained control rule is applied to the plant, and the cycle repeats. Let consider the Eq. (3) without seismic excitation term as

$$\begin{aligned} x_{k+1} &= Ax_k + Bu_k \\ y_k &= C_d \times x_k \end{aligned} \tag{4}$$

Based on Eq. (4) the future output variables are

calculated sequentially using the set of future control parameters

$$Y_{k+i|k} = Fx_k + \theta u_k \tag{5}$$

Where the subscript $k+i|k$ denotes the value of a predicted variable at the future time $k+i$ based on the knowledge of the system at time k, $Y_{k+i|k}=\begin{bmatrix} y_{k+1|k} \\ y_{k+2|k} \\ \vdots \\ y_{k+p|k} \end{bmatrix}$, $F=\begin{bmatrix} C_dA \\ C_dA^2 \\ \vdots \\ C_dA^p \end{bmatrix}$, $\theta = \begin{bmatrix} C_dB & 0 & \cdots & 0 & 0 \\ C_dAB & C_dB & & 0 & 0 \\ \vdots & & \ddots & \vdots & \\ C_dA^{p-1}B & C_dA^{p-2}B & \cdots & C_dA^{p-c}B & \end{bmatrix}$, p and c are the prediction and control horizons, respectively.

For a given constant reference trajectory at a time step, the objective of the MPC is to approximate the predicted output to the reference trajectory. This objective is then transformed to an optimization problem to find the best control parameter.

Therefore, the quadratic cost function to be minimized is defined as follows

$$\underset{u_k}{Min} J_p(Y_k,u) = (R_s - Y_k)^T \bar{Q}(R_s - Y_k) + u_k^T \bar{R} u_k \tag{6a}$$

Subject to

$$Du_{k+i|k} \le d \tag{6b}$$

Where R_s is the reference trajectory, D is the input constraint matrix and d is corresponding constraint values for input constraint. The matrices $\bar{Q} \ge 0$ and $\bar{R} \ge 0$ are positive semi-definite weighting matrices. In this paper, the constrained optimization problem is solved using Hildreth's quadratic programming method (Wang 2009). The corresponding control rule is obtained by solving the Eqs. (6a)-(6b) as follows

$$u_k = (B^T \bar{Q} B + \bar{R})^{-1} B^T \bar{Q}(R_s - Fx_k) \tag{6c}$$

4. Developed model predictive control

As mentioned earlier, the objective of this study is to propose a developed MPC scheme such that the extracted control rule to be more accurate than the conventional MPC. For this purpose, a seismic excitation model is needed to be embedded in the MPC formulation.

Determining a mathematical model for seismic excitation model provides the possibility of estimating future ground accelerations. In the case of conventional MPC, the concluded control rule is only based on the dynamic properties of the structures, while in the developed case, the future ground accelerations imposed on the structures are also considered to extract the optimal control rule.

In this section, at first, a forecasting seismic excitation model is formulated based on the online learning of two AR models, then an optimal state estimation method (in this research KF) is depicted to apply to the problem. An online learning and noise elimination method (in this study RLS) is discussed in continue, and finally, an algorithm is suggested.

4.1 Seismic excitation model

The ground acceleration can be modeled as an autoregressive (AR) model as follows

$$\ddot{x}_{g_k} = \phi_1 \ddot{x}_{g_{k-1}} + \phi_2 \ddot{x}_{g_{k-2}} + \cdots + \phi_n \ddot{x}_{g_{k-n}} \tag{7}$$

In which $\ddot{x}_g$ is ground acceleration, φ is the model coefficient and n is the number of variables. In this paper, the AR model is described as a binomial equation.

Rewriting Eq. (7) in the binomial format and expanding it to the future steps, the following equations are obtained

$$\begin{aligned} \ddot{x}_{g_k} &= \phi_1 \ddot{x}_{g_{k-1}} + \phi_2 \ddot{x}_{g_{k-2}} \\ \ddot{x}_{g_{k+1}} &= \phi_1 \ddot{x}_{g_k} + \phi_2 \ddot{x}_{g_{k-1}} \\ &= \phi_1\left(\phi_1 \ddot{x}_{g_{k-1}} + \phi_2 \ddot{x}_{g_{k-2}}\right) + \phi_2 \ddot{x}_{g_{k-1}} \\ &\vdots \\ \ddot{x}_{g_{k+p}} &= (\phi_1^{p+1} + \cdots)\ddot{x}_{g_{k-1}} + (\phi_1^{p+1}\phi_2 + \cdots)\ddot{x}_{g_{k-2}} \end{aligned} \tag{8}$$

Rewriting in the matrix form

$$\ddot{X}_{gf} = \varphi \times \ddot{X}_{gp} \tag{9}$$

Where, $\ddot{X}_{gf}=\begin{bmatrix} \ddot{x}_{g_k} \\ \ddot{x}_{g_{k+1}} \\ \vdots \\ \ddot{x}_{g_{k+p}} \end{bmatrix}$, $\Phi = \begin{bmatrix} \varphi_1 & \varphi_2 \\ \varphi_1^2 + \varphi_2 & \varphi_1\varphi_2 \\ \vdots & \vdots \\ \varphi_1^{p+1} + \ldots & \varphi_1^p\,\varphi_2 + \ldots \end{bmatrix}$, $\ddot{X}_{gp}=\begin{bmatrix} \ddot{x}_{g_{k-1}} \\ \ddot{x}_{g_{k-2}} \end{bmatrix}$.

Since the Eq. (9) contains an uncertainty in the prediction of higher steps due to the stochastic nature of the earthquakes, so, in this method, another AR model is formulated to predict the errors between predicted and measured ground accelerations for p sequential steps as follows

$$Er_{gf} = B^* \times Er_{gp} \tag{10}$$

Where $B^*=\begin{bmatrix} \beta_{1,1} & \cdots & \beta_{1,p} \\ \vdots & \ddots & \vdots \\ \beta_{p,1} & \cdots & \beta_{p,p} \end{bmatrix}$, $Er_{gp} = \begin{bmatrix} \ddot{x}_{g_{k+1-p}} - \ddot{x}_{g_{m+1-p}} \\ \ddot{x}_{g_{k+2-p}} - \ddot{x}_{g_{m+2-p}} \\ \vdots \\ \ddot{x}_{g_k} - \ddot{x}_{g_m} \end{bmatrix}$, and $Er_{gf} = \begin{bmatrix} \ddot{x}_{g_{k+1}} - \ddot{x}_{g_{m+1}} \\ \ddot{x}_{g_{k+2}} - \ddot{x}_{g_{m+2}} \\ \vdots \\ \ddot{x}_{g_{k+p}} - \ddot{x}_{g_{m+p}} \end{bmatrix}$.

In which, m is related to measured data, and β is the coefficients correlating errors between predicted and measured data in the p previous and next steps. It is worth noting that the Eqs. (9) and (10) are computed in an online

manner.

Then, the Eq. (5) can be rewritten as follows

$$Y_{k+i|k} = Fx_k + \theta u_k + V(\ddot{X}_{gf} + Er_{gf}) \tag{11}$$

Where $V = \begin{bmatrix} C_dG & 0 & \cdots & 0 & 0 \\ C_dAG & C_dG & & 0 & 0 \\ \vdots & & \ddots & \vdots & \\ C_dA^{p-1}G & C_dA^{p-2}G & \cdots & C_dA^{p-c}G & \end{bmatrix}$.

Substituting Eq. (11) in Eqs. (6a)-(6b) the resulted control rule is achieved as follows

$$u_k = (B^T\bar{Q}B + \bar{R})^{-1}B^T\bar{Q}\begin{pmatrix} R_s - Fx_k \\ -V(\ddot{X}_{gf} + Er_{gf}) \end{pmatrix} \tag{12}$$

4.2 Kalman Filter

Estimating the exact states of the controlled systems has always been a significant issue. Since the measurement devices (i.e., sensors) because of some imperfections in their structures are not able to measure the system states perfectly, providing a solution to attenuate the problem can be effective. So, in this research, the Kalman Filter (KF) algorithm is utilized in the proposed control process to achieve a more accurate control procedure.

Kalman filter is an algorithm that uses both noisy measurements and inaccurate system models to estimates unknown variables with more accuracy. The algorithm consists of two different stages; in the first stage, also known as the prediction stage, the next step of states is predicted based on the system model. In the second stage, also known as the update stage, accurate estimates are obtained integrating both measurements and predictions. The algorithm formulation is as follows (Simon 2006)

$$y_k = H_kx_k + \nu_k \tag{13a}$$

$$\hat{x}_k^- = F_{k-1}\hat{x}_{k-1}^+ + G_{k-1}u_{k-1} \tag{13b}$$

$$P_k^- = F_{k-1}P_{k-1}^+F_{k-1}^T + Q_{k-1} \tag{13c}$$

$$K_k = P_k^-H_k^T(H_kP_k^-H_k^T + R_k)^{-1} = P_k^+H_k^TR_k^{-1} \tag{13d}$$

$$\hat{x}_k^+ = \hat{x}_k^- + K_k(y_k - H_k\hat{x}_k^-) \tag{13e}$$

$$\begin{aligned} P_k^+ &= (I - K_kH_k)P_k^-(I - K_kH_k)^T + K_kR_kK_k^T \\ &= [(P_k^-)^{-1} + H_k^TR_k^{-1}H_k]^{-1} = (I - K_kH_k)P_k^- \end{aligned} \tag{13f}$$

Where y is measurement vector, H is observation model, ν is measurement noise, x is the true state, $\hat{x}^-$ is predicted state, $\hat{x}^+$ is updated state, F is state transition model, G is the control-input model; u is input, p^- is predicted state covariance, p^+ is updated state covariance, Q is process noise covariance, K is optimal Kalman gain, and R is measurement noise covariance.

4.3 Recursive least squares

Recursive least squares is the recursive application of the least square algorithm in which the previous parameters of a linear correlation is updated as the new data is received. The algorithm formulation is as follows (Gibbs 2011)

$$K_k = P_k^-H_k^T(H_kP_k^-H_k^T + \lambda R_k)^{-1} \tag{14a}$$

$$\hat{x}_k^+ = \hat{x}_k^- + K_k(y_k - H_k\hat{x}_k^-) \tag{14b}$$

$$P_k^+ = (I - K_kH_k)P_k^-/\lambda \tag{14c}$$

As it is clear, the RLS is the update step of the KF. The only difference between the KF and RLS is the forgetting factor (λ) considered in RLS. This factor has a range between 0 and 1. With $\lambda = 1$, all the data are given identical weight in the solution, and with $\lambda \ll 1$, only the most recent data are given much weight in the solution. In this study, the RLS method is utilized for two different purposes: (1) parameter estimation of the autoregressive model (section 4.1), (2) noise elimination of measured ground acceleration.

The design procedure of the DPMC based on sections 4.1-4.3 is summarized by Algorithm 1.

5. Numerical examples

In this paper, the numerical examples are the three- and nine-story benchmark SAC buildings (Ohtori *et al*. 2006). These benchmark buildings have been designed and developed by the American Society of Civil Engineers (ASCE) Committee on structural control for the comparison of control algorithms in building structures. The mentioned buildings are perimeter steel moment resistant frame (SMRF) buildings that meet the seismic code requirement of the 1994 UBC for the Los Angeles, California, region. In this study, the buildings are considered as the shear frames with a linear behavior. Comprehensive details about the

Algorithm 1.
DMPC design procedure

Step 1. Use the RLS method for the noise elimination of data received from ground acceleration (Eqs. (14a)-(14c)).
Step 2. Construct a seismic excitation model using the AR model (Eq. (9)).
Step 3. Construct an error compensator model for step 2 using the AR model (Eq. (10)).
Step 4. Determine the parameters of (Eq. (9)) and (Eq. (10)) using the RLS method (Eqs. (14a)-(14c)).
Step 5. Estimate the states of the system using KF (Eqs. (13a)-(13f)).
Step 6. Integrate (Eq. (9)), (Eq. (10)), and (Eq. (5)) to form (Eq. (11)).
Step 7. Substitute (Eq. (11)) in (Eqs. (6a)-(6b)) to obtain the DMPC control rule (Eq. (12)).
Step 8. Repeat the procedure as the new data is received.

building's specifications can be found in Ohtori *et al*. (2004). Furthermore, an ATMD is located on the top story of the buildings for vibration control of them. The ATMD mass and damping ratios are considered to be 2% of the building total mass and 5%, respectively. The weighting matrices are also chosen to be Q = diag $[q_{d1}, q_{td1}\ q_{v1}, q_{tv1}, \ldots, q_{d5}, q_{td5}\ q_{v5},\ q_{tv5}]$ for which q_{d1}= 1000 × $I_{(9\times9)}$, q_{v1}= 10 × $I_{(9\times9)}$, q_{td1} & q_{tv1}= 1e-3, $q_{d2,3,4,5}$= 1 × $I_{(9\times9)}$, $q_{v2,3,4,5}$= 1 × $I_{(9\times9)}$, $q_{td2,3,4,5}$ & $q_{tv2,3,4,5}$= 1e-5, R = 1e-10 × $I_{(5\times5)}$, for the nine-story building and q_{d1}= 10 × $I_{(3\times3)}$, q_{v1}= 1 × $I_{(3\times3)}$, q_{td1} & q_{tv1}= 1e-5, $q_{d2,3,4,5}$= 1 × $I_{(3\times3)}$, $q_{v2,3,4,5}$= 1 × $I_{(3\times3)}$, $q_{td2,3,4,5}$ & $q_{tv2,3,4,5}$= 1e-8, R = 1e-11 × $I_{(5\times5)}$ for the three-story building. diag stands for diagonal matrix and I is identity matrix.

The input rate changes and input constraints are considered for actuator saturation simulation. These constraints for input rate changes and input constraints are assumed to be 200 and 500 KN respectively .Furthermore, the optimal control problem is solved in a receding-horizon manner. The number of prediction (p) and control (c) horizons are also assumed to be 5.

The efficiency of the proposed method is evaluated utilizing two far-field (El Centro & Hachinohe) and two near-field (Kobe & Northridge) earthquake records. The absolute peak accelerations of the El Centro, Hachinohe, Northridge, and Kobe records are 3.417, 2.250, 8.267, and 8.178 m/sec^2, respectively (Ohtori *et al*. 2004).

6. Numerical results

In this section, the responses of the three- and nine-story benchmark buildings are evaluated by applying two near-field and two far-field earthquakes. The third floor of the three-story and the ninth floor of the nine-story buildings are selected to demonstrate under the two earthquake records (El Centro as a far-field earthquake and Kobe as a near-field earthquake) and different control strategies including uncontrolled and active-controlled cases. The active control strategy is also comprised of three different strategies, including ideal, proposed, and conventional MPC. In the ideal MPC, the data of the applied earthquake records are supposed to be already known. Performance indices also play an important role in the evaluation of the responses. Therefore, twelve performance indices are defined to evaluate the responses in Table 1. These indices are controlled to uncontrolled response ratios and include max drift ratio (J_1), max story acceleration (J_2), max story velocity (J_3), max story displacement (J_4), max base shear (J_5), max control force (J_6), RMS of drift ratio (J_7), RMS of story acceleration (J_8), RMS of story velocity (J_9), RMS of story displacement (J_{10}), RMS of base shear (J_{11}), and RMS of control force (J_{12}).

6.1 Three-story building

The displacement time history responses of the third floor under the two earthquake records (El Centro & Kobe) are shown in Figs. 1(a)-(b). The displacement responses of the building under the near-field (Kobe) and far-field (El Centro) earthquakes demonstrate the better conformity of the proposed MPC with the ideal one. The responses also show the efficiency of the controlled cases in reducing the responses of the building. It is worth noting that, the reason for the greater responses in the proposed and ideal control methods than the conventional one is the use of the same weighting matrices that are designed for the conventional method.

Figs. 2(a)-(b), demonstrate the velocity and acceleration RMS time histories of the third floor. The better conformity of the proposed method for both the El Centro and Kobe earthquakes is concluded from the figures. The maximum drift ratio responses of the three-story building for all of the

Table 1 Performance indices

Max drift ratio	Max story acceleration	Max story velocity
$J_1(q)=\frac{\left\\|{}^{max}_{t,f}\lvert\delta_c(t,q,f)\rvert\right\\|}{\left\\|{}^{max}_{t,f}\lvert\delta_{uc}(t,q,f)\rvert\right\\|}$	$J_2(q)=\frac{\left\\|{}^{max}_{t,f}\lvert\ddot{x}_c(t,q,f)\rvert\right\\|}{\left\\|{}^{max}_{t,f}\lvert\ddot{x}_{uc}(t,q,f)\rvert\right\\|}$	$J_3(q)=\frac{\left\\|{}^{max}_{t,f}\lvert\dot{x}_c(t,q,f)\rvert\right\\|}{\left\\|{}^{max}_{t,f}\lvert\dot{x}_{uc}(t,q,f)\rvert\right\\|}$
Max story displacement	Max base shear	Max control force
$J_4(q)=\frac{\left\\|{}^{max}_{t,f}\lvert x_c(t,q,f)\rvert\right\\|}{\left\\|{}^{max}_{t,f}\lvert x_{uc}(t,q,f)\rvert\right\\|}$	$J_5(q)=\frac{\left\\|{}^{max}_{t}\lvert V_c(t,q)\rvert\right\\|}{\left\\|{}^{max}_{t}\lvert V_{uc}(t,q)\rvert\right\\|}$	$J_6(q)=\frac{\left\\|{}^{max}_{t}\lvert U_c(t,q)\rvert\right\\|}{\left\\|{}^{max}_{i}\lvert W\rvert\right\\|}$
RMS drift ratio	RMS story acceleration	RMS story velocity
$J_7(q)=\frac{\left\\|{}^{RMS}_{t,f}\lvert\delta_c(t,q,f)\rvert\right\\|}{\left\\|{}^{RMS}_{t,f}\lvert\delta_{uc}(t,q,f)\rvert\right\\|}$	$J_8(q)=\frac{\left\\|{}^{RMS}_{t,f}\lvert\ddot{x}_c(t,q,f)\rvert\right\\|}{\left\\|{}^{RMS}_{t,f}\lvert\ddot{x}_{uc}(t,q,f)\rvert\right\\|}$	$J_9(q)=\frac{\left\\|{}^{RMS}_{t,f}\lvert\dot{x}_c(t,q,f)\rvert\right\\|}{\left\\|{}^{RMS}_{t,f}\lvert\dot{x}_{uc}(t,q,f)\rvert\right\\|}$
RMS story displacement	RMS base shear	RMS control force
$J_{10}(q)=\frac{\left\\|{}^{RMS}_{t,f}\lvert x_c(t,q,f)\rvert\right\\|}{\left\\|{}^{RMS}_{t,f}\lvert x_{uc}(t,q,f)\rvert\right\\|}$	$J_{11}(q)=\frac{\left\\|{}^{RMS}_{t}\lvert V_c(t,q)\rvert\right\\|}{\left\\|{}^{RMS}_{t}\lvert V_{uc}(t,q)\rvert\right\\|}$	$J_{12}(q)=\frac{\left\\|{}^{RMS}_{t}\lvert U_c(t,q)\rvert\right\\|}{\left\\|{}^{RMS}_{i}\lvert W\rvert\right\\|}$

*Note: f = Story number, 1, ….,*Ni* (*Ni* = 9); q = earthquake number; c = controlled cases including ideal, proposed, and conventional MPC ; *u*c = uncontrolled case; t = time; ||•|| = 2- norm operator; |•| = absolute value operator. RMS = root mean square; max = maximum; δ = drift ratio; $\ddot{x}$ = acceleration; $\dot{x}$ =velocity; x =displacement; V = base shear; U = control force; W = structural whole weight

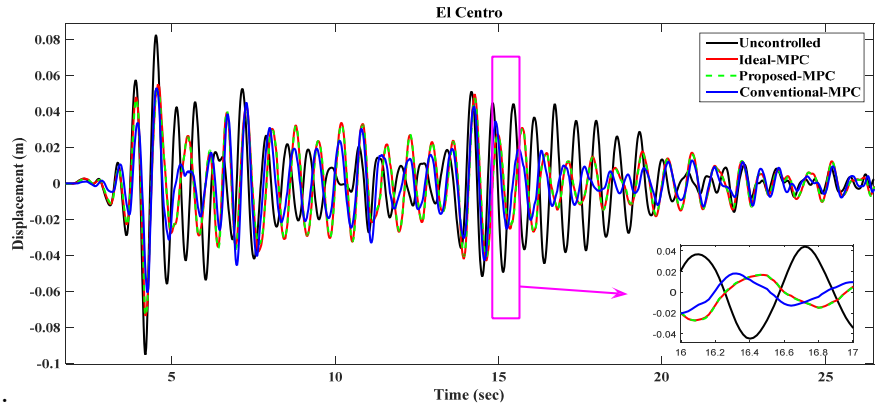

(a)

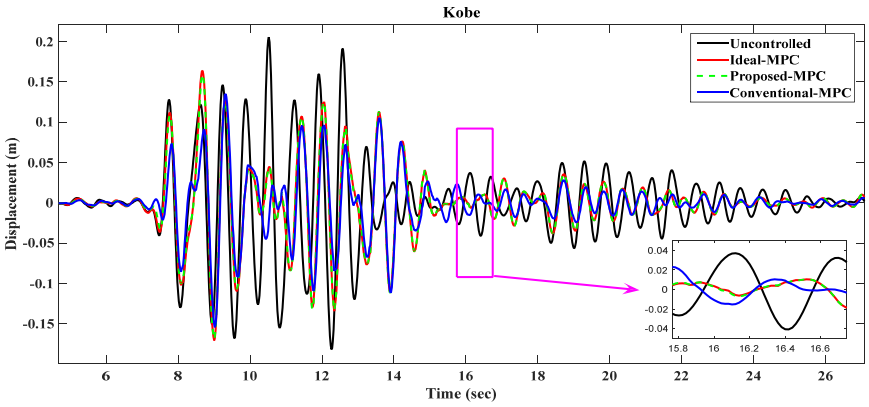

(b)

Fig. 1 Displacement time histories of the three-story building for the El Centro (a) and Kobe (b) earthquakes. Third story

floors are depicted in Figs. 3(a)-(b). It should be noted that, using the proposed method leads to better responses (conformity) in all of the cases. Better base shear conformity is also verified in the proposed method for both the earthquake records in Fig. 4.

Control force is one of the most important responses of the study. The conformity of the control force in the proposed method with the ideal one is demonstrated in Figs. 5(a)-(b). The actuator saturation is also detected in the Kobe earthquake.

The values of the defined indices are obtained using mentioned control approaches. These values are demonstrated in Table 2. The performance indices show the higher conformity of the proposed method with the ideal

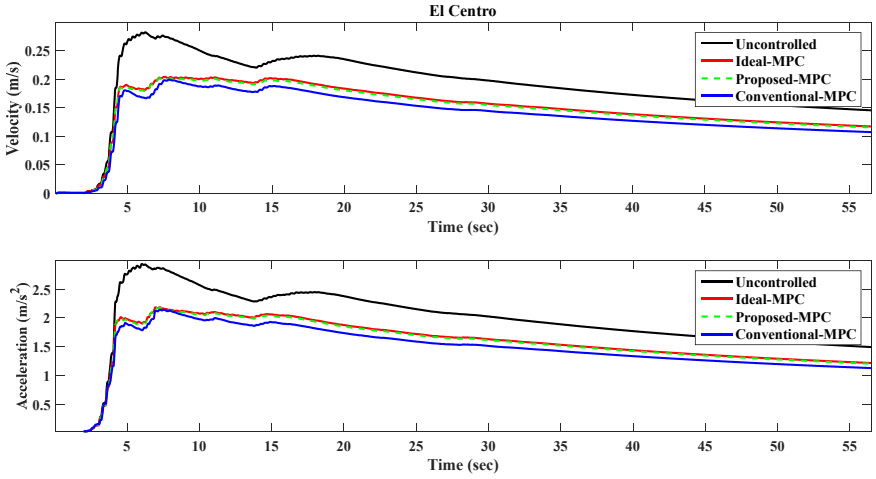

(a)

Fig. 2 Velocity and acceleration RMS time histories of the three-story building for the El Centro (a) and Kobe (b) earthquakes. Third story

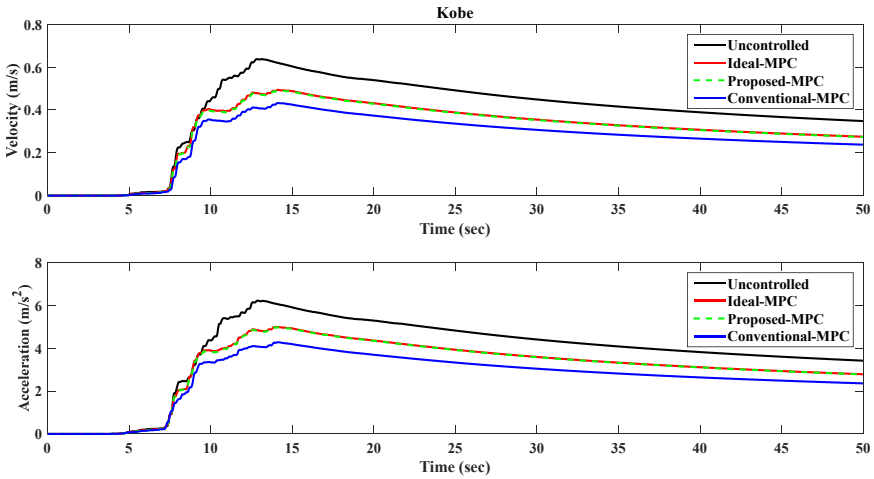

(b)

Fig. 2 Continued

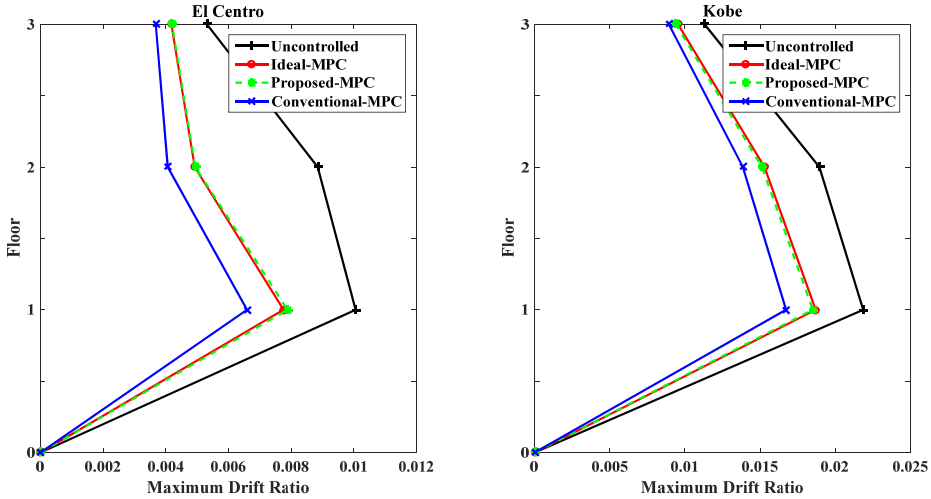

Fig. 3 Maximum drift ratios of the three-story building for the El Centro and Kobe earthquakes

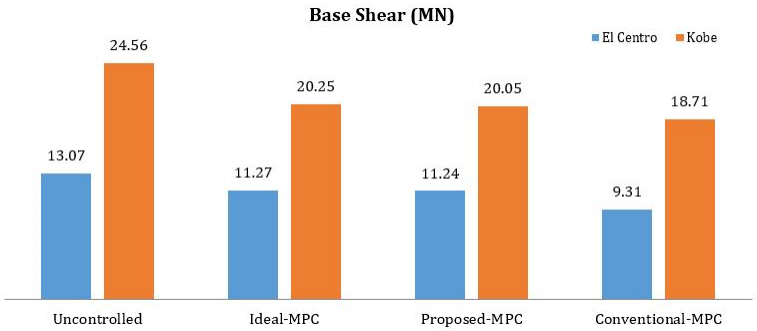

Fig. 4 Base shear of the three-story building for the El Centro and Kobe earthquakes

one almost in all of the cases. The most conformity difference among the performance indices is related to the RMS control force (J_{12}) for the Hachinohe record such that the conformity of the proposed method with the ideal one is by up to 91% more than the conformity of the conventional method with the ideal one. The least conformity difference is also related to the maximum control force (J_6) for the applied control force constraints for the Hachinohe record with a value of 0%. The average conformity values of all the performance indices for the proposed method are also by up to 21%, 20%, 21%, and 9% more than the conventional one for El Centro, Hachinohe, Northridge, and Kobe earthquake records, respectively.

The rest of the indices indicate the better conformity of the proposed MPC with the ideal one. It means that the proposed MPC is a more accurate control approach than the

Table 2 Performanve indices variations for three-story building

		Performance Indices											
Earthquakes	Cases	J_1	J_2	J_3	J_4	J_5	J_6	J_7	J_8	J_9	J_{10}	J_{11}	J_{12}
El Centro	CMPC	0.531	0.696	0.788	0.637	0.712	0.003	0.718	0.801	0.738	0.697	0.839	0.001
	DMPC	0.628	0.831	0.763	0.776	0.86	0.017	0.851	0.811	0.786	0.813	0.884	0.002
	IMPC	0.626	0.825	0.774	0.775	0.862	0.015	0.873	0.812	0.797	0.834	0.885	0.002
Hachinohe	CMPC	0.686	0.917	0.784	0.745	0.941	0.001	0.638	0.772	0.684	0.624	0.781	0
	DMPC	0.671	0.847	0.834	0.764	0.929	0.006	0.756	0.726	0.696	0.748	0.738	0.002
	IMPC	0.673	0.836	0.818	0.793	0.909	0.006	0.757	0.714	0.692	0.75	0.726	0.002
Northridge	CMPC	0.538	0.868	0.827	0.676	0.895	0.004	0.675	0.906	0.744	0.676	0.937	0.001
	DMPC	0.731	0.939	0.823	0.883	0.995	0.027	0.76	0.84	0.766	0.75	0.847	0.003
	IMPC	0.744	0.941	0.823	0.898	1.002	0.023	0.793	0.828	0.766	0.786	0.832	0.003
Kobe	CMPC	0.747	0.695	0.78	0.752	0.762	0.035	0.642	0.751	0.687	0.619	0.8	0.008
	DMPC	0.807	0.786	0.846	0.826	0.816	0.035	0.78	0.827	0.786	0.76	0.849	0.008
	IMPC	0.817	0.785	0.856	0.834	0.825	0.035	0.794	0.827	0.789	0.774	0.85	0.008

*Note: CMPC = conventional model predictive control; DMPC = developed model predictive control (proposed method); IMPC = ideal model predictive control

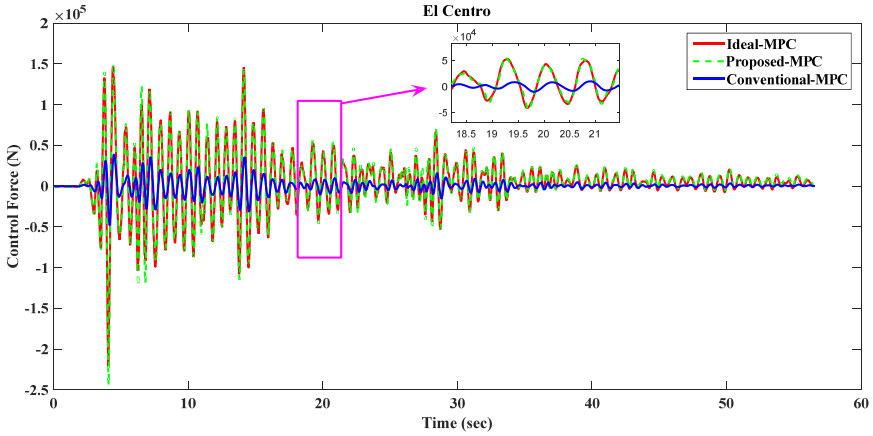

(a)

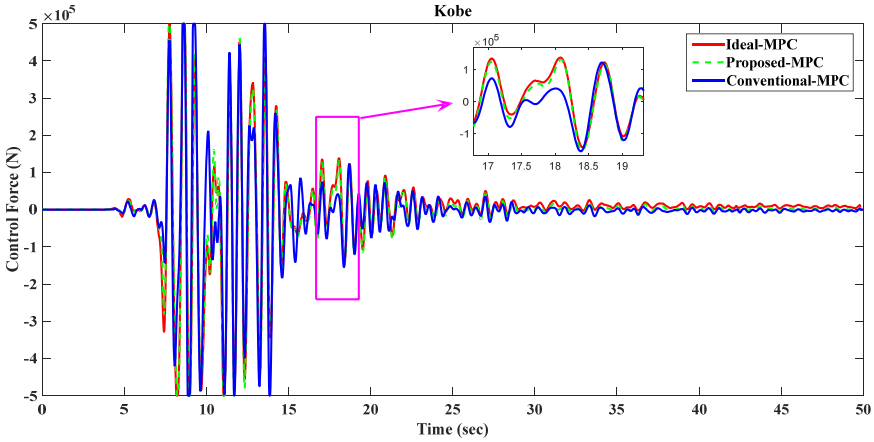

(b)

Fig. 5 Control force time histories of the three-story building for the El Centro (a) and Kobe (b) earthquakes

conventional MPC.

According to the results obtained in Table 2, the indices are appropriately reduced in the majority of the cases. The value of these indices also expresses the suitability of the applied control method.

The displacement time history responses of the ninth

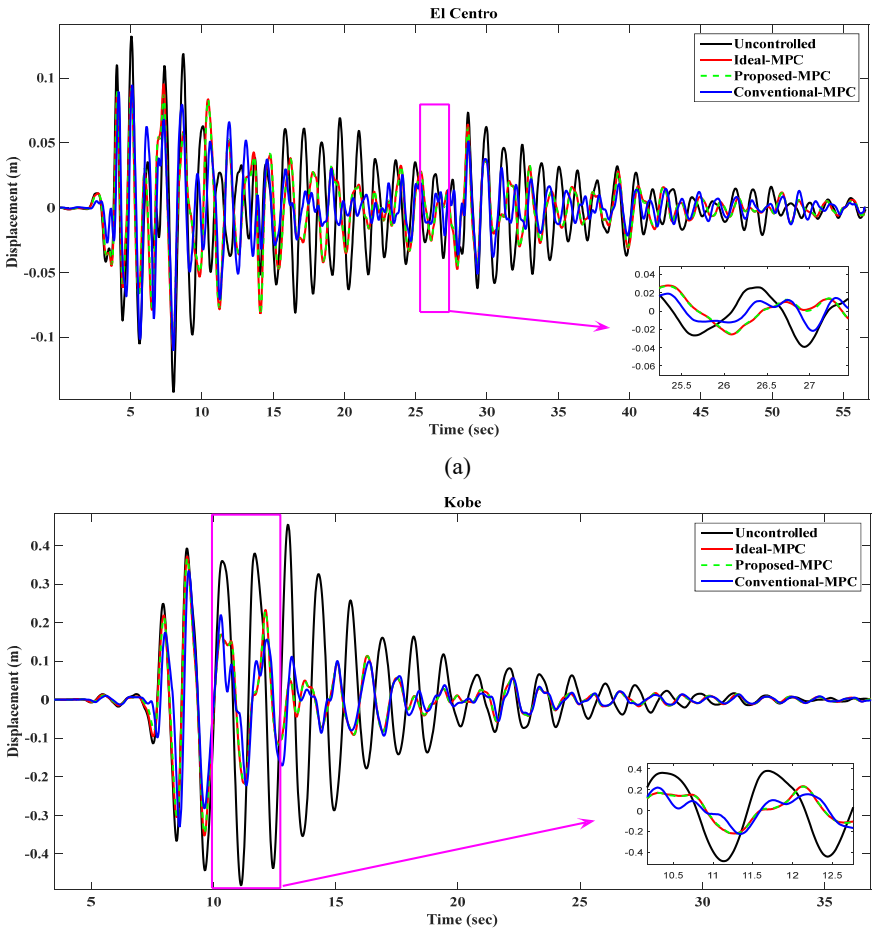

Fig. 6 Displacement time histories of the nine-story building for the El Centro (a) and Kobe (b) earthquakes. Ninth story

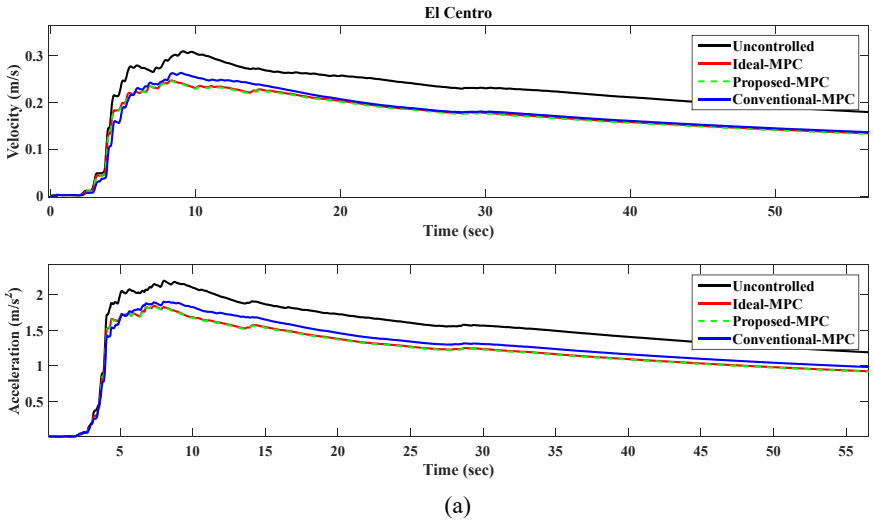

Fig. 7 Velocity and acceleration RMS time histories of the nine-story building for the El Centro (a) and Kobe (b) earthquakes. Ninth story

floor under the far-field (El Centro) and near-field (Kobe) records are shown in Figs. 6(a)-(b). The displacement responses of the nine-story building under both the earthquakes demonstrate the better conformity of the proposed MPC with the ideal one. As mentioned earlier, it is possible to have fewer responses in the proposed and ideal methods than the conventional one by tuning the weighting matrices.

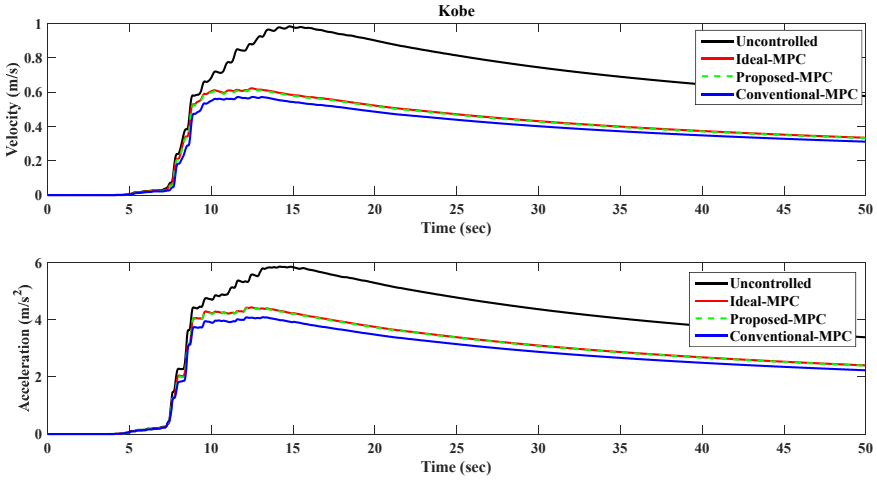

(b)

Fig. 7 Continued

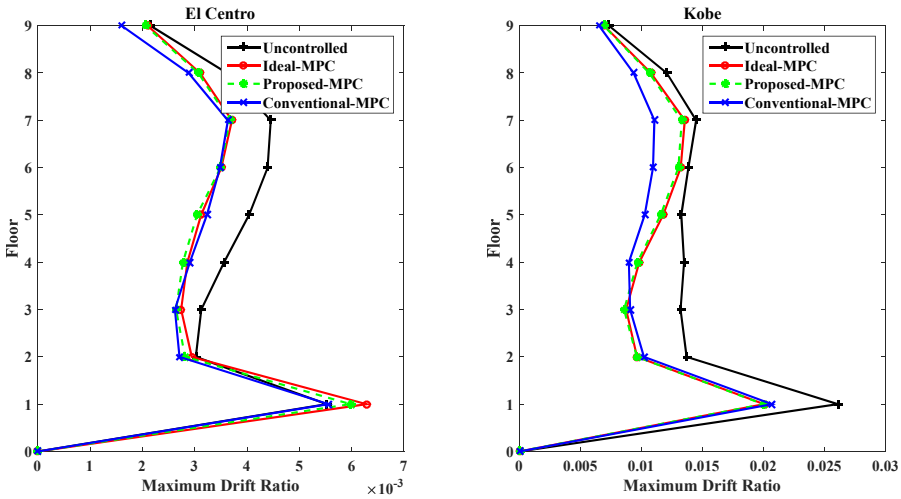

Fig. 8 Maximum drift ratios of the nine-story building for the El Centro and Kobe earthquakes

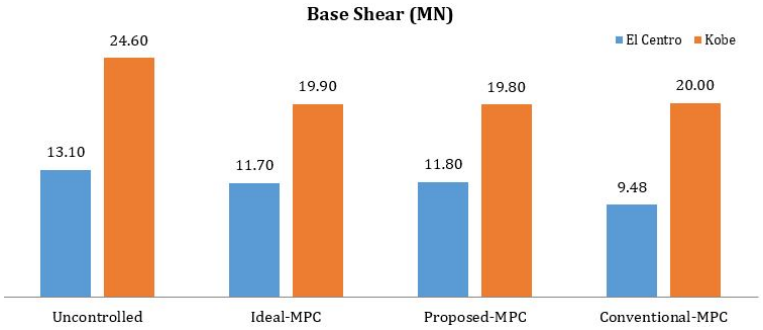

Fig. 9 Base shear of the nine-story building for the El Centro and Kobe earthquakes

6.2 Nine-story building

Figs. 7(a)-(b), demonstrate the velocity and acceleration RMS time histories of the ninth floor. The better conformity of the proposed method for both the El Centro and Kobe earthquakes is concluded from the figures.

The maximum drift ratio responses of the nine-story building for all of the floors are depicted in Figs. 8(a)-(b). It should be noted that using the proposed method leads to better responses in all of the cases. Better base shear conformity is also verified in the proposed method for both the earthquake records in Fig. 9. The conformity of the control force in the proposed method with the ideal one is demonstrated in Figs. 10(a)-(b). The actuator saturation is also detected in the Kobe earthquake.

The values of the defined indices are obtained using the

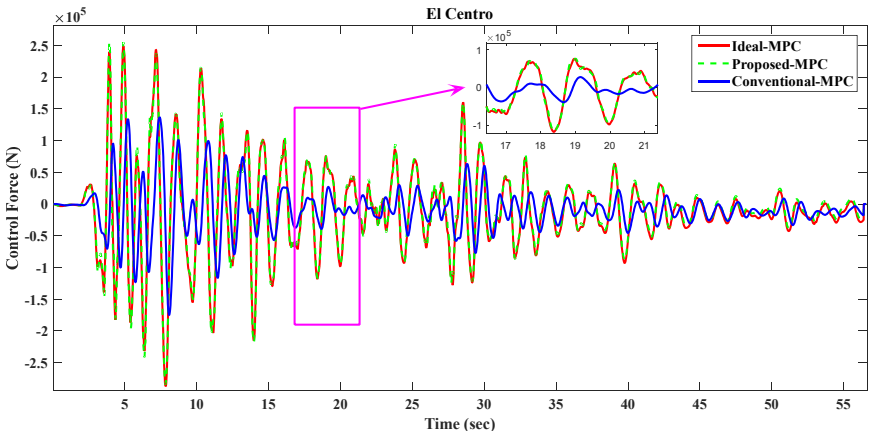

(a)

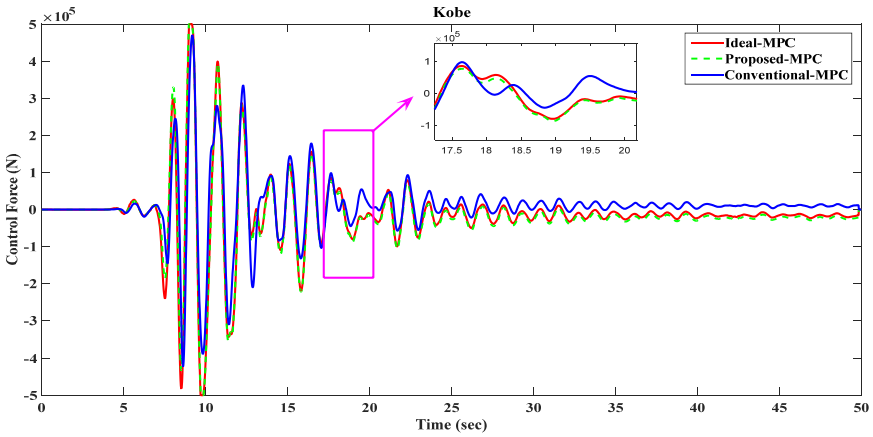

(b)

Fig. 10 Control force time histories of the nine-story building for the El Centro (a) and Kobe (b) earthquakes

Table 3 Performanve indices variations for nine-story building

		Performance Indices											
Earthquakes	Cases	J_1	J_2	J_3	J_4	J_5	J_6	J_7	J_8	J_9	J_{10}	J_{11}	J_{12}
El Centro	CMPC	0.814	1.03	0.854	0.789	1.093	0.004	0.71	0.917	0.778	0.706	0.91	0.001
	DMPC	0.825	0.972	0.833	0.807	0.97	0.006	0.775	0.865	0.745	0.737	0.865	0.002
	IMPC	0.842	0.959	0.815	0.819	0.954	0.007	0.791	0.86	0.753	0.756	0.855	0.002
Hachinohe	CMPC	0.815	1.081	0.772	0.804	1.101	0.006	0.808	0.992	0.883	0.803	0.987	0.002
	DMPC	0.848	1.046	0.876	0.855	0.955	0.006	0.872	0.969	0.911	0.883	0.937	0.002
	IMPC	0.833	1.034	0.871	0.841	0.934	0.006	0.871	0.959	0.908	0.883	0.926	0.002
Northridge	CMPC	0.718	0.826	0.772	0.622	0.756	0.011	0.706	0.83	0.738	0.666	0.827	0.003
	DMPC	0.893	0.97	0.873	0.861	0.935	0.011	0.826	0.879	0.803	0.797	0.881	0.004
	IMPC	0.92	0.984	0.876	0.894	0.958	0.011	0.853	0.881	0.813	0.827	0.885	0.004
Kobe	CMPC	0.751	0.929	0.893	0.705	1.067	0.011	0.512	0.739	0.532	0.469	0.718	0.002
	DMPC	0.826	0.952	0.955	0.717	0.944	0.011	0.561	0.761	0.579	0.516	0.707	0.002
	IMPC	0.838	0.956	0.958	0.724	0.92	0.011	0.568	0.76	0.584	0.525	0.703	0.002

*Note: CMPC = conventional model predictive control; DMPC = developed model predictive control (proposed method); IMPC = ideal model predictive control

mentioned control approaches. These values are demonstrated in Table 3. The performance indices show the higher conformity of the proposed method with the ideal one in all of the cases. The most conformity difference among the performance indices is related to the RMS control force (J_{12}) for El Centro record such that the conformity of the proposed method with the ideal one is by up to 46% more than the conformity of the conventional

method with the ideal one. The least conformity difference is also related to the max control force (J_6) for applied control forceconstraints for Northridge record with a value of 0%. The average conformity values of all the performance indices for the proposed method are also by up to 11%, 5%, 13%, and7% more than the conventional one for El Centro, Hachinohe, Northridge and Kobe records, respectively.

The rest of the performance indices values also indicate the better conformity of the proposed MPC with the ideal one. It means that the proposed MPC is a more accurate control approach than the conventional MPC.

According to the results obtained in Table 3, the indices are appropriately reduced in the majority of the cases. The value of these indices also expresses the suitability of the applied control method.

7. Conclusions

In this paper, a developed version of MPC approach is proposed and implemented. This proposed method is based on the prediction of seismic excitation applied to the building. For this purpose, two AR model for seismic excitation is formulated and updated in an online manner as the new data is received. The RLS method is utilized for two different purposes: (1) parameters estimation of the AR models; (2) noise elimination of the measured ground acceleration. The KF is also used as an optimal estimator for the state estimation of the model. Furthermore, two near-field and two far-field earthquake records are selected and applied to the three- and nine-story benchmark buildings to evaluate the efficiency of the proposed method. The applied active control strategy is comprised of three different strategies, including ideal, proposed, and conventional MPC. The performance criterion of the proposed method is the conformity of the responses compared to the ideal MPC. So, the performance of the proposed control method is studied through the twelve benchmark performance indices. The numerical simulation results demonstrate the better conformity of the responses obtained from the proposed method with those obtained from the ideal one in all of the cases. The average conformity values of all the performance indices in the case of three-story building for the proposed method are also by up to 21%, 20%, 21%, and 9% more than the conventional one for El Centro, Hachinohe, Northridge, and Kobe earthquake records, respectively. These conformity values are also 11%, 5%, 13%, and 7% more than the conventional one for El Centro, Hachinohe, Northridge, and Kobe records in the case of the nine-story building, respectively.

The overall results of numerical simulations indicate that the proposed method is an effective approach to increase the accuracy of the conventional MPC subjected to the earthquake events.

References

Chen, Y., Zhang, S., Peng, H., Chen, B. and Zhang, H. (2017), "A novel fast model predictive control for large - scale structures", *J. Vib. Control*, **23**(13), 2190-2205. https://doi.org/10.1177/1077546315610033

Farina, M., Giulioni, L. and Scattolini, R. (2016), "Stochastic linear model predictive control with chance constraints–a review", *J. Process. Control.*, **44**, 53-67. https://doi.org/10.1016/j.jprocont.2016.03.005

Gharebaghi, S.A. and Zangooeia, E. (2017), "Chaotic particle swarm optimization in optimal active control of shear buildings", *Struct. Eng. Mech., Int. J.*, **61**(3), 347-357. https://doi.org/10.12989/sem.2017.61.3.347

Gibbs, B.P. (2011), *Advanced Kalman Filtering, Least-squares and Modeling: A Practical Handbook*, John Wiley & Sons, NJ, USA.

Heirung, T.A., Paulson, J.A., O'Leary, J. and Mesbah, A. (2018), "Stochastic model predictive control—how does it work?", *Comput. Chem. Eng.*, **114**, 158-170. https://doi.org/10.1016/j.compchemeng.2017.10.026

Katebi, J. and Jangara, J. (2020), "Application of adaptive sliding mode control (sigma adaption method) for an uncertain three-story benchmark structure", *Adv. Struct. Eng.*, **23**(3), 497-509. https://doi.org/10.1177/1369433219875306

Katebi, J. and Zamen, S. (2018), "Robust time varying sliding sector for uncertain structures control", *J. Vib. Control.*, **24**(1), 171-190. https://doi.org/10.1177/1077546316636540

Khodabandehlou, H., Pekcan, G., Fadali, M.S. and Salem, M.M. (2018), "Active neural predictive control of seismically isolated structures", *Struct. Control. Health Monit.*, **25**(1), e2061. https://doi.org/10.1002/stc.2061

Kim, B., Washington, G.N. and Yoon, H.S. (2013), "Active vibration suppression of a 1D piezoelectric bimorph structure using model predictive sliding mode control", *Smart. Struct. Syst., Int. J.*, **11**(6), 623-635. https://doi.org/10.12989/sss.2013.11.6.623

Lana, C. and Rotea, M. (2008), "Desensitized model predictive control applied to a structural benchmark problem", *IFAC Proceedings Volumes*, **41**(2), 13188-1393. https://doi.org/10.3182/20080706-5-KR-1001.02234

Lee, J.H. (2014), "From robust model predictive control to stochastic optimal control and approximate dynamic programming: A perspective gained from a personal journey", *Comput. Chem. Eng.*, **70**, 114-121. https://doi.org/10.1016/j.compchemeng.2013.10.014

Luo, J., Jin, K., Wang, M., Yuan, J. and Li, G. (2017), "Robust entry guidance using linear covariance-based model predictive control", *Int. J. Adv. Robot. Syst.*, **14**(1), 1729881416687503. https://doi.org/10.1177/1729881416687503

Mei, G., Kareem, A. and Kantor, J.C. (2001), "Real-time model predictive control of structures under earthquakes", *Earthq. Eng. Struct. Dyn.*, **30**(7), 995-1019. https://doi.org/10.1002/eqe.49

Mei, G., Kareem, A. and Kantor, J.C. (2002), "Model predictive control of structures under earthquakes using acceleration feedback", *J. Eng. Mech.*, **128**(5), 574-585. https://doi.org/10.1061/(ASCE)0733-9399(2002)128:5(574)

Mei, G., Kareem, A. and Kantor, J.C. (2004), "Model predictive control of wind-excited building: Benchmark study", *J. Eng. Mech.*, **130**(4), 459-465. https://doi.org/10.1061/(ASCE)0733-9399(2004)130:4(459)

Mesbah, A. (2016), "Stochastic model predictive control: An overview and perspectives for future research", *IEEE Control. Syst. Mag.*, **36**(6), 30-44. https://doi.org/10.1109/MCS.2016.2602087

Mayne, D. (2016), "Robust and stochastic model predictive control: Are we going in the right direction?", *Annu. Rev. Control.*, **41**, 184-192. https://doi.org/10.1016/j.arcontrol.2016.04.006

Moghaddasie, B. and Jalaeefar, A. (2019), "Optimization of LQR

method for the active control of seismically excited structures", *Smart. Struct. Syst.*, *Int. J.*, **23**(3), 243-261. https://doi.org/10.12989/sss.2019.23.3.243

Ohtori, Y., Christenson, R.E., Spencer, Jr. B.F. and Dyke, S.J. (2004), "Benchmark control problems for seismically excited nonlinear buildings", *J. Eng. Mech.*, **130**(4), 366-385. https://doi.org/10.1061/(ASCE)0733-9399(2004)130:4(366)

Pnevmatikos, G.N. (2012), "New strategy for controlling structures collapse against earthquakes", *Nat. Sci.*, **4**, 667-676. http://dx.doi.org/10.4236/ns.2012.428088

Pnevmatikos, G.N. and Gantes, J.C. (2011), "The influence of time delay and saturation capacity in control of structures under seismic excitations", *Smart. Struct. Syst.*, *Int. J.*, **8**(5), 449-470. http://dx.doi.org/10.12989/sss.2011.8.5.449

Patan, K. (2018), "Two stage neural network modelling for robust model predictive control", *ISA. Trans.*, **72**, 56-65. https://doi.org/10.1016/j.isatra.2017.10.011

Peng, H., Li, F., Zhang, S. and Chen, B. (2017), "A novel fast model predictive control with actuator saturation for large-scale structures", *Comput. Struct.*, **187**, 35-49. https://doi.org/10.1016/j.compstruc.2017.03.014

Peng, H., Chen, Y., Li, E., Zhang, S. and Chen, B. (2018), "Explicit expression-based practical model predictive control implementation for large-scale structures with multi-input delays", *J. Vib. Control.*, **24**(12), 2605-2620. https://doi.org/10.1177/1077546316689341

Peng, H., Li, F. and Kan, Z. (2020), "A novel distributed model predictive control method based on a substructuring technique for smart tensegrity structure vibrations", *J. Sound. Vib.*, **471**, 115171. https://doi.org/10.1016/j.jsv.2020.115171

Seron, M.M., Goodwin, G.C. and Carrasco, D.S. (2019), "Stochastic model predictive control: Insights and performance comparisons for linear systems", *Int. J. Robust. Nonlinear. Control.*, **29**(15), 5038-5057. https://doi.org/10.1002/rnc.4106

Simon, D. (2006), *Optimal State Estimation: Kalman*, *H Infinity*, *and Nonlinear Approaches*, John Wiley & Sons, NJ, USA.

Wang, L. (2009), *Model predictive control system design and implementation using MATLAB®*, Springer Science & Business Media, London, England.

Xu, L.H. and Li, Z.X. (2011), "Model predictive control strategies for protection of structures during earthquakes", *Struct. Eng. Mech.*, *Int. J.*, **40**(2), 233-243. https://doi.org/10.12989/sem.2011.40.2.233

Yang, C.S., Chung, L.L., Wu, L.Y. and Chung, N.H. (2011), "Modified predictive control of structures with direct output feedback", *Struct. Control. Health. Monit.*, **18**(8), 922-940. https://doi.org/10.1002/stc.411

CC